Scale-up Effect of Riser Reactors: Particle Velocity and Flow Development

Aijie Yan and Jesse (Jingxu) Zhu
Dept. of Chemical and Biochemical Engineering, University of Western Ontario, London, Ontario, Canada N6A 5B9

DOI 10.1002/aic.10556
Published online August 8, 2005 in Wiley InterScience (www.interscience.wiley.com).

The influence of riser diameter on the axial and radial particle velocity profiles and flow development is studied in a 10 m high twin-riser system (76- and 203-mm ID risers). Cross-sectional average particle velocity is somewhat lower for the larger riser with a steeper radial particle velocity profile. The flow development in the riser center is nearly instant with the particle velocity remaining high. There is no significant difference for the two risers in the center region. In the wall region, the flow development is significantly slower and the particle velocity of the smaller riser is higher. The flow development slows down in the larger riser. In all locations measured, there was a clear dependency between the local particle velocity and solids concentration of both risers. Gas distribution and particle aggregation are considered the key factors that influence the local hydrodynamics in the twin-riser system. © 2005 American Institute of Chemical Engineers *AIChE J,* 51: 2956–2964, 2005

Keywords: circulating fluidized bed, particle velocity profile, flow development, riser diameter, five-fiber optic probe

Introduction

Gas–solid reactions take place in a wide range of chemical processes, such as circulating fluidized bed (CFB) combustion and fluid-catalytic cracking (FCC). Because of their use in petroleum refineries for FCC, circulating fluidized beds were "reinvented"[1,2] in the late 1970s. Since then, intensive studies have been carried out to improve these industrial processes. FCC units are used in most refineries all over the world to convert high molecular weight gas oils or residuum charge stocks into lighter hydrocarbon products in a riser reactor within a few seconds. However, a shorter and a more uniform catalyst residence time in the riser reactor would potentially lead to a better reaction performance (larger amounts of desired products and/or a higher conversion). That is, because coke deposition rapidly deactivates the catalyst leading to reduced selectivity and some desirable products (gasoline, light olefins, light cycle oil) may further react to cause over-cracking. These non-beneficial factors could be limited or avoided by having more uniform axial and radial particle flow structure in the riser, leading to shorter and more uniform solids as well as gas residence times.

To apply fundamental knowledge from pilot scale risers into a commercial riser, it is necessary to achieve a clear understanding of the scale-up effects. Extensive research has been carried out on CFB riser reactors.[3-17] Although there were some researches on particle velocity in the literature,[3-5,7,9,12,17,18] most data were taken in risers of small diameter ($<$0.15 m) and / or short length ($<$7 m). Considering most industrial risers are of 1 m or larger in diameter and of 20 m or taller in height, it is not reliable to base the industrial design on the experimental results obtained in small diameter and very short risers since small diameter vessels are dominated by wall effects and the entrance and exit structures have great influence on the short height vessels. It is very important to understand the scale-up effect on the hydrodynamics inside the risers of significant sizes. Unfortunately, no previous studies have been published with respect to gas and particle flow over a wide range of operating conditions in risers of different diameters. Therefore, more research on the influence of riser diameter on particle

Correspondence concerning this article should be addressed to J. Zhu at jzhu@uwo.ca.

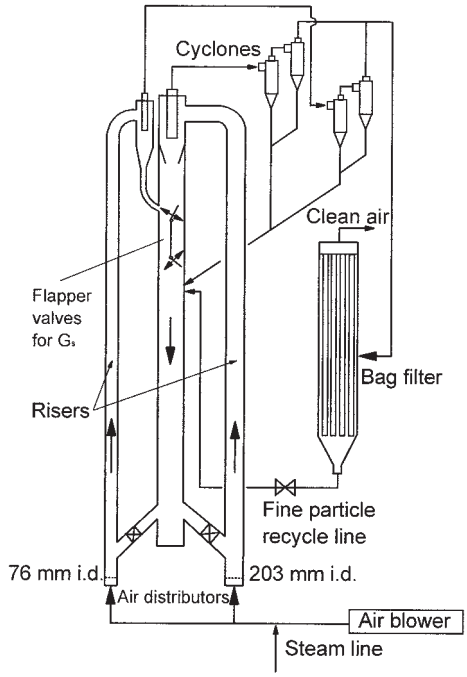

Figure 1. Twin-riser circulating fluidized bed apparatus.

velocity distribution and flow development is required in large-scale CFB risers to improve and optimize the existing industrial CFBs and enhance the design for novel applications.

To minimize the possibility of expensive errors in scaling-up to commercial operation, and to optimize and improve the designs of existing industrial FCC riser reactors, a good understanding of the scale-up obtained from pilot-scale risers, such as the knowledge of the particle flow distribution in CFB risers of significant size, is necessary. This work used a twin-riser system, with two 10 m long riser units having internal diameters (ID) of 76 mm (3 in.) and 203 mm (8 in.) and otherwise having identical geometries (sharing the same downcomer and air supply, using the same particles), over a wide range of operating conditions with the solids circulation rate up to 200 kg m^{-2} s^{-1} and superficial gas velocity up to 8.0 m/s. The influence of riser diameter on the axial and radial particle velocity profiles and flow development is carefully studied by measuring the local particle velocity with an optical-fiber probe along the twin-riser system. The information obtained from this study could be beneficial, especially for the FCC industry.

Experimental Apparatus

The experiments were conducted in a twin-riser circulating fluidized bed system shown schematically in Figure 1, consisting of two 10 m long risers, 76- and 203-mm IDs, which use the same downcomer (storage tank) of ID 0.32 m. FCC catalyst with a mean diameter of 67 μm and a particle density of 1500 kg/m^3 were used. The total solids inventory was about 350 kg, equivalent to a solids level of nearly 5 m in the downcomer. The humidity level of the air was controlled between 70 and 80% to minimize the effect of electrostatics in the system.

The configurations (except for the diameter) are identical for both risers. The relative dimensions of the inlet and outlet openings to the diameters are equal to the corresponding diameter. After passing through a short inclined pipe section, where a flip valve was installed to control the solids flow rate, the solids from the storage tank entered the riser bottom at a height of 0.21 m in each riser and were accelerated by air in near-ambient conditions (at the base of the riser, the temperature is about 20°C and absolute pressure is about 105.7 kPa). After initial mixing and accelerating, the gas–solids suspension traveled up in the column and passed through a smooth exit into the primary cyclone for gas–solids separation, and escaped solids entered into the secondary and tertiary cyclones, with the final gas–solids separation carried out by a bag filter. Two separate sets of cyclones were used for each riser, although the two risers shared the same bag filter. Only one riser operated at a given time. From the bottom of the large-capacity bag filter, collected fine particles could be returned to the downcomer. The solids flow rate measuring device located in the top portion of the downcomer sectioned the column into two halves with a central vertical plate and with two half-butterfly valves fixed at the top and the bottom of the two-half section. By appropriately flipping over the two valves from one side to the other, solids circulated through the system can be accumulated in one side of the measuring section for a given time period to provide the solids circulation rate.

A five-fiber optic velocity probe was inserted into the column to measure the particle velocity. Each of the five fibers is a silicon optical fiber of diameter 200 μm. The probe consists of a horizontal cylindrical portion of diameter 2 mm and length about 0.3 m, leading to a 10 mm long tip having an oval-shaped cross section of 0.5 $\times$ 1.8 mm (width $\times$ height). The five-fiber optic probe consists of two light-emitting fibers (B and D) and three light-detecting fibers (A, C, and E) arranged precisely in the same vertical line. A particle flowing by the center point between any two neighboring fibers will produce a reflective signal to a detection fiber. By counting the time difference between the two signals from A–B and B–C (or C–D and D–E), the velocity of a particle passing along the array of the five fibers can be determined. More details of the five-fiber optic probe have been presented by Zhu et al.[19] The particle velocity was measured at 11 radial positions (r/R = 0.00, 0.16, 0.38, 0.50, 0.59, 0.67, 0.74, 0.81, 0.87, 0.92, and 0.98) on eight axial levels (Z = 1.53, 2.73, 3.96, 5.13, 5.90, 6.34, 8.74, and 9.42 m) for the 76-mm ID riser and five axial levels (Z = 1.47, 2.69, 3.91, 5.90, and 8.79 m) for the 203-mm ID riser under several operating conditions as given in Table 1. At each measurement location the sampling time was typically >30 s and the amount of sampled particles > 2500.

The local solids concentration was measured with a reflective-type fiber-optic concentration probe. The 3.8 mm diameter probe tip consisted of nearly 8000 emitting and receiving quartz fibers, each having a diameter of 15 μm. The active area, where the fibers were located, was about 2 $\times$ 2 mm. More

Table 1. Operating Conditions

76-mm ID Riser		203-mm ID Riser	
U_g (m/s)	G_s (kg m^{-2} s^{-1})	U_g (m/s)	G_s (kg m^{-2} s^{-1})
5.5	50	5.5	50
3.5	100	5.5	75
5.5	100	5.5	100
8.0	100	8.0	100
5.5	200		

details of this probe can be found in Zhang et al.,[20] and more details of the concentration probe measurements from the same twin-riser system can be found in Yan and Zhu.[21] The solids concentration was measured in the same positions and at the same operating conditions as the particle velocity. Two samples were taken at each location, and the total sampling time was 60 s. By combining the results from the current study with those of Yan and Zhu,[21] the cross-sectional net solids fluxes were obtained for each axial elevation. Those were found to be in a good agreement with the results from the solids flow rate measuring device (G_s) in the downcomer (within 10–15%). The cross-sectionally mean solids holdups were obtained by averaging the local solids holdups measured at 10 radial positions (excluding the center point) with the fiber-optic concentration probe at each axial elevation.

Results and Discussion

Development of radial profiles of particle velocity

In our study, we used large-scale CFB risers (with diameters up to 0.2 m and bed height of 10 m to ensure that the particle flow is fully developed in the riser) with high gas velocity (up to 8 m/s) to study the influence of bed diameter on radial profiles of the particle velocities. Figure 2a shows the radial profiles of particle velocity on eight axial elevations of the 76-mm ID riser under five operating conditions. The solids circulation rates were 50, 100, and 200 kg m^{-2} s^{-1} and the superficial gas velocities were 3.5, 5.5, and 8.0 m/s. Radial profiles of particle velocity on five axial elevations of the 203-mm ID riser under four operating conditions are shown in Figure 2b. The solids circulation rates were 50, 75, and 100 kg m^{-2} s^{-1} and the superficial gas velocities were 5.5 and 8.0 m/s. In general, the particle velocities are more uniform in the upper section than in the lower section of the riser at all radial positions and higher in the center than in the wall region of the riser at all axial locations. Figure 2 also shows that the particle velocity in the center region of the riser remains nearly constant throughout the riser under each operating condition for both risers, and then decreases toward the wall. Figure 2 further shows that the particle velocity in the center region of the riser does not seem to change significantly under the same superficial velocity within the tested range of operating conditions for both risers. As a result, the flow development is mostly represented by the increase of the particle velocity toward the riser top at r/R from about 0.50 to 1.00. In the riser bottom, the particle velocity drops significantly toward the wall. Toward the riser top, the particle velocity in the wall region tends to increase. Increasing the superficial gas velocity U_g increases the particle velocity throughout the riser. The solids circulation rate (overall solids flux) G_s seems to have only a slight influence on the value of particle velocity. In addition, the radial profile of particle velocity seems more uniform with lower solids flux. That is, increasing solids flux slows down the flow development. Similar phenomena were also observed in the radial particle velocity profiles of the same 76-mm ID riser under higher flux operating conditions as shown in Pärssinen and Zhu.[17] Because of the limitation of the capacity of the storage tank, the solids flux in the 203-mm ID riser cannot reach a very high flux. It will be our future work to study higher flux conditions in the 203-mm ID riser after modifying the equipment to increase the capacity of the storage tank.

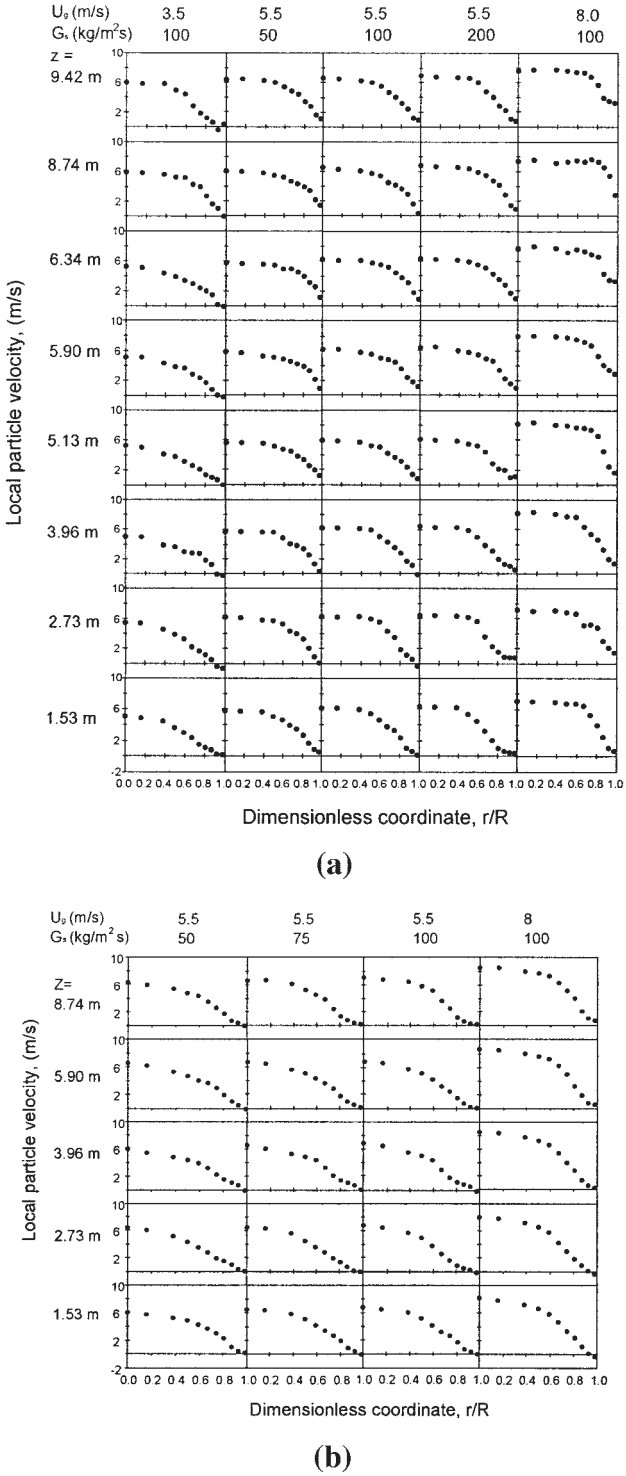

Figure 2. (a) Radial profiles of local particle velocity under five operating conditions on eight axial levels of the 76-mm ID riser, showing the flow development along the riser; (b) radial profiles of local particle velocity under four operating conditions on five axial levels of the 203-mm ID riser, showing the flow development along the riser.

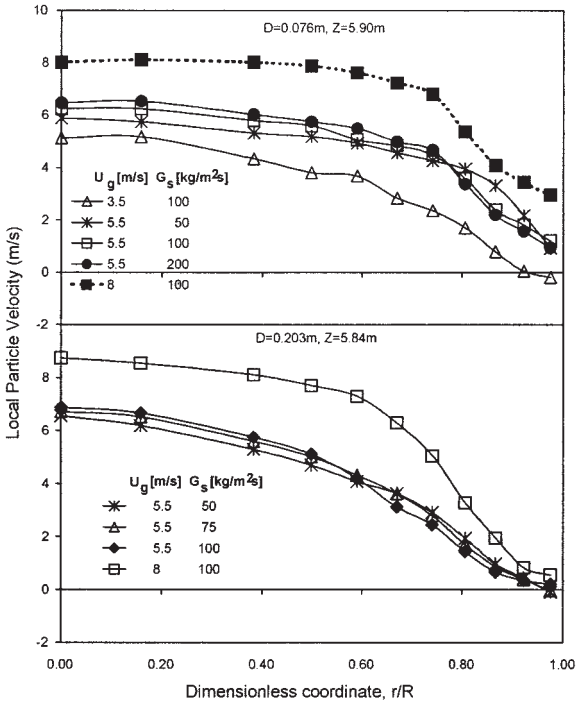

Figure 3. Comparison of the typical radial profiles of local particle velocity in the same five axial levels for the risers.

Figure 2 also shows the flow development with respect to the radial profiles of particle velocity under each operating condition in the 10 m high twin-riser system. At the bottom section ($Z = 1.53$ and/or 2.73 m), the radial profile shows a flat center region, turning then smoothly downward toward the wall, and having a fairly wide wall region with a velocity value of <2 m/s. This may be referred to as a horizontal "S"-shape. In the upper levels, the solids accelerate more in the radial region of $r/R = 0.0$ to 0.4, leading to a combination of linear (but not flat) and parabolic-shaped radial velocity profile. When the solids reach the exit section, the particles slow down somewhat, and the corresponding velocity profiles become scattered as a result of the exit features as the solids pass through the 90 ° smooth elbow. Observed from Figure 2, it seems that the flow development in the 203-mm ID riser is considerably slower than that of the 76-mm ID riser. The shape change of the radial profiles of the 203-mm ID riser also happens at a much higher level than that of the 76-mm ID riser. This is because of the scale-up effect, which will be discussed later in more detail.

Figure 3 provides the typical radial profiles of particle velocity for both risers at $Z = 5.90$ m. Figure 3 also shows that increasing U_g tends to make the radial profiles more uniform. There is little influence of solids flux on the radial distributions of particle velocity, which is likely a consequence of the quicker flow development under lower flux, in agreement with the observations from Figure 2. Similar tendencies are observed in the other axial levels. Zhou et al.[18] also observed that, under lower flux conditions, increasing solids circulation rate leads to steeper radial profiles for particle velocity.

By comparing the velocity profiles at 1.53, 2.73, and 3.96 m (marked as closed symbols with connecting lines), Figure 4 shows that increasing U_g from 5.5 to 8.0 m/s (with $G_s = 100$ kg m^{-2} s^{-1}) causes a faster flow development. On the other hand, increasing G_s seems to slow down the flow development slightly under a constant U_g of 5.5 m/s. The flow development at higher flux is slower, as observed under higher flux operating conditions in the same riser as shown in Pärssinen and Zhu.[17] It is also observed in Figure 4 that the shape change of the radial profiles of the 203-mm ID riser is at a much higher level than that of the 76-mm ID riser.

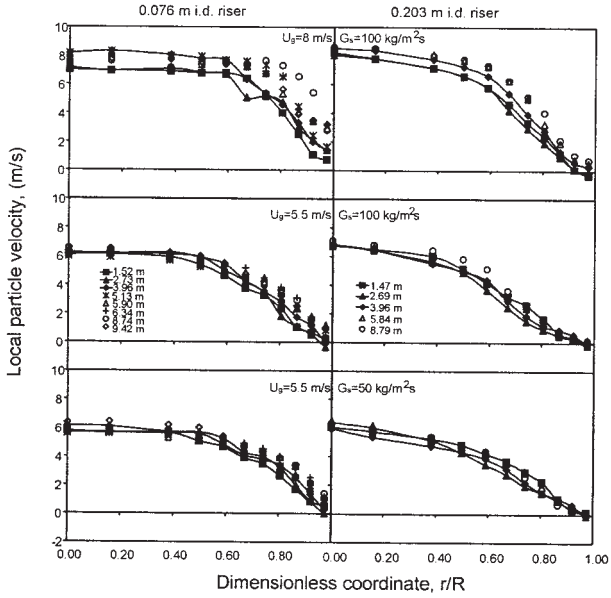

Figure 4. Comparison of the development of radial profiles of local particle velocities for the risers.

When observing the radial profiles of the riser from the bottom to the top, it is also seen that the flow develops first in the riser center region, and then gradually and progressively closer to the wall as the solids pass through the riser. This can be seen more clearly in Figure 5, which plots the particle velocities in three radial regions on eight axial elevations in the 76-mm ID riser and five axial elevations in the 203-mm ID riser (the particle velocity in each region is obtained by aver-

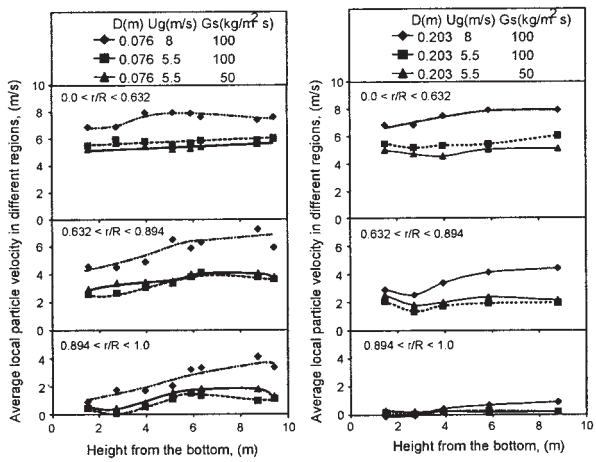

Figure 5. Comparison of the average particle velocities in different radial regions along the riser under all three operating conditions for the risers.

aging the local particle velocities in that region). In this figure, the difference in the flow development in the three radial regions is clearly revealed. Furthermore, the scale-up effect on the flow development is also clearly observed. In the center region of the riser ($0.0 < r/R < 0.632$, 40% of the cross-sectional area), the particles already gained a fairly high velocity before the height of 1.5 m, whereas a maximum velocity is finally reached at the height of 3–4 m. There is no significant difference for the two risers in this region. In the middle region ($0.632 < r/R < 0.894$, 40% of the cross-sectional area), on the other hand, the particle velocity is increasing throughout the riser, and the increase is more obvious with higher gas velocity. Meanwhile, the particle velocity of the 76-mm ID riser increases more sharply than that of the 203-mm ID riser in this middle region. That is, increasing riser diameter slows down the flow development. In the wall region ($0.894 < r/R < 1.0$, 20% of the cross-sectional area), the particle velocity remains low up to about 4–6 m and then increases slowly toward the riser top. The flow development in this region is significantly slower than that in the two other regions. Moreover, it is also clearly shown that the particle velocity of the 203-mm ID riser increases much less than that of the 76-mm ID riser in this region. From the riser bottom to the top, the radial distribution of the 76-mm ID riser becomes uniform much earlier than that of the 203-mm ID riser. Thus, the flow development slows down with large riser. Figure 5 also indicates that increasing gas velocity significantly enhances the flow development (that is, to cause particles to accelerate quicker and at lower levels in the riser). The same tendency was also observed under higher flux operating conditions in the same 76-mm ID riser as shown in Pärssinen and Zhu[17]; however, the flow development of higher flux conditions is much slower, especially in the middle region.

In Figure 5, the particle velocities from the riser bottom to the top in the center region are almost the same and change only slightly along the riser. However, the differences of particle velocities from the riser bottom to the top at the middle and wall regions are much more obvious. Figure 5 clearly shows that particle acceleration (and therefore flow development) first starts from the center and then extends to the wall. This dictates the development of the radial profiles of particle velocity. In the bottom section, only those particles in the center region had some acceleration so that the horizontal S-shape appears. In the middle section, particles in the middle radial region start to accelerate so that the particle velocity in this region increases, resulting in the combination of linear (but not flat) and parabolic-shape profile. In the exit section, particles in the middle region accelerate further to catch up with those particles in the center region, and particles in the wall region also begin to accelerate, leading to a parabolic radial profile. Because the flow development slows down when the riser diameter is scaled-up, the shape change of the radial profiles of the 203-mm ID riser happens at a much higher level than that of the 76-mm ID riser, as also observed in Figures 2 and 4.

Figure 6, which compares the radial profiles of particle velocity between the 76- and the 203-mm ID risers, indicates that there is a slight difference in the center region of radial profiles of the two risers. However, it is quite different in the wall region. The radial distributions of particle velocity of the 76-mm ID riser are comparably more uniform and less sensitive to the change of the axial position than that of the 203-mm ID riser. The difference is mainly a result of riser diameter difference. This may be explained by some secondary effects, such as the introduction of the solids to the side at the base of the riser, poor dispersion of solids in the riser, or the shorter *L/D* in the larger-diameter vessel. Further research is needed for these secondary effects. Figure 7 compares the radial solids holdup profiles of the twin-riser system at $Z = 5.84$ m. It is shown that the solids holdup of the 203-mm ID riser at each radial position is higher than that of the 76-mm ID riser under the same operating conditions and at the same axial level, especially in the wall region. In an earlier paper[21] by the same authors reporting on the axial and radial solids concentration distribution, similar results can also be observed in the other axial levels. That is, under the same solids circulation rate and gas velocity, a larger riser has a larger solids concentration at each radial position, especially in the wall region. This shows a much more substantial wall effect, even in the relative magnitude, for the larger-diameter riser. A denser concentration of solids occupies the wall region of the large-diameter riser and restricts the gas flow at the wall. As a result, the particle velocity tends to be lower in the wall region for the larger-diameter riser. To maintain the cross-sectional U_g, the gas velocity has to be correspondingly higher in the center region of the large riser. A higher gas velocity in the center could also lead to higher particle velocities. Again, this verified the scale-up effect of risers on the flow development: increasing riser diameter impedes flow development.

Figure 8a shows the variation of particle velocity in the wall region with the cross-sectional mean solids holdup, obtained by

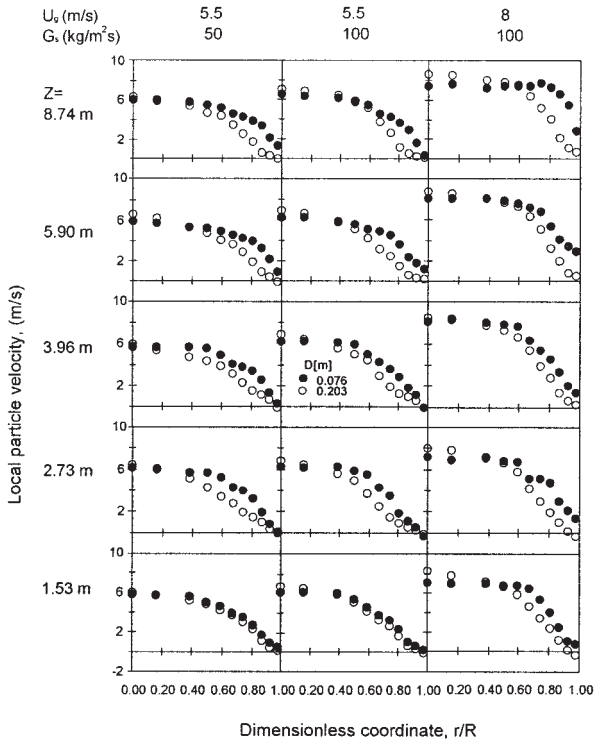

Figure 6. Comparison of the radial profiles of local particle velocity for the risers of different diameters.

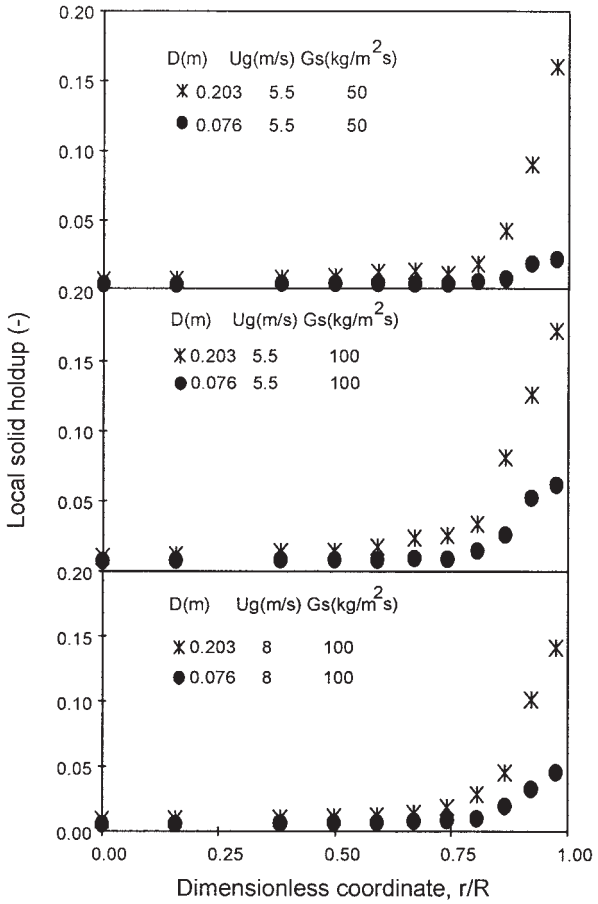

Figure 7. Comparison of radial profiles of local solids holdup the twin-riser system at $Z = 5.84$ m.

averaging the local solids holdups measured at 10 radial positions (excluding the center point) with the fiber-optic concentration probe at each axial elevation, at each axial level of the 76-mm ID riser. For this 76-mm ID riser, with a high cross-sectional mean solids concentration (riser bottom), the particle velocity at the wall region is relatively low. With a lower cross-sectional solids concentration (riser top), the particle velocities are higher at the wall region. A simple regression provides the following correlation between the particle velocity at the wall region and the cross-sectional average solids holdup of the 76-mm ID riser

$$V_{p,wall} = -0.98 \ln(\bar{\varepsilon}_s) - 2.23 \quad (0 < \bar{\varepsilon}_s < 0.42,\ V_p > -1.38 \text{ m/s}) \quad (1)$$

This correlation is very close to that obtained from the higher flux conditions of the same 76-mm ID riser.[17] The particle velocity in the wall region of the 203-mm ID riser could also be related to the cross-sectional solids concentration at each axial level, as shown in Figure 8b. However, the relationship between the particle velocity in the wall region and the cross-sectional solids concentration of the 203-mm ID riser is different from that of the 76-mm ID riser. As mentioned earlier, because of the slow flow development of the large riser, the cross-sectional solids concentrations of the 203-mm ID riser are relatively higher, so that the particle velocities near the wall are lower than those of the 76-mm ID riser at the same axial level. Therefore, as shown in Figure 8, no data appeared in the range of very low cross-sectional solids holdup and high particle velocity for the wall region of the 203-mm ID riser. The particle velocity in the wall region and the cross-sectional solids holdup of the 203-mm ID riser are more clustered together than that of the 76-mm ID riser.

Comparison of the axial development of particle velocities in the twin-riser system

Figure 9 compares the axial profiles of the one-dimensional (cross-sectional average) particle velocities on each axial level obtained with the fiber-optic velocity (Figure 9a) and with the concentration (Figure 9b) probes under the same operating conditions for both risers. In Figure 9a, the local particle velocity was weighted with the local solids holdup in each

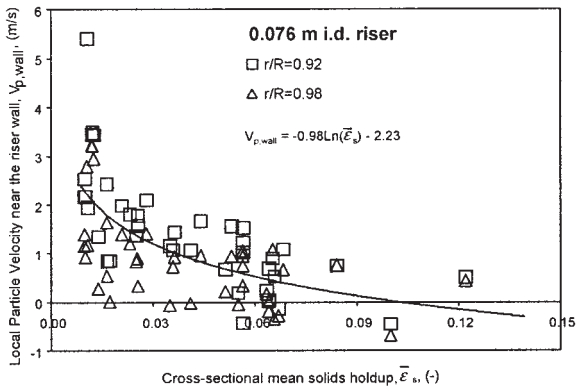

(a)

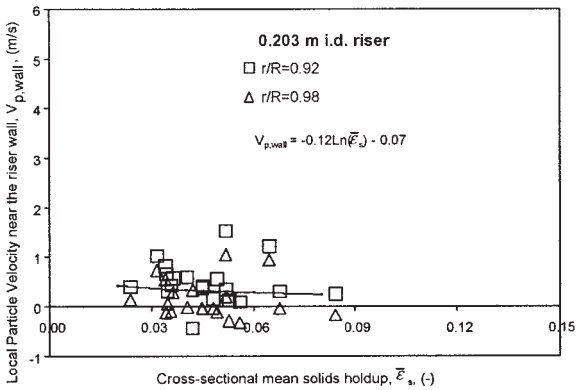

(b)

Figure 8. (a) Relationship between the local particle velocity near the riser wall ($r/R = 0.92$ and 0.98) and the cross-sectional mean solids holdup on all axial elevations under all measured operating conditions for the 76-mm ID riser; (b) relationship between the local particle velocity near the riser wall ($r/R = 0.92$ and 0.98) and the cross-sectional mean solids holdup on all axial elevations under all measured operating conditions for the 203-mm ID riser.

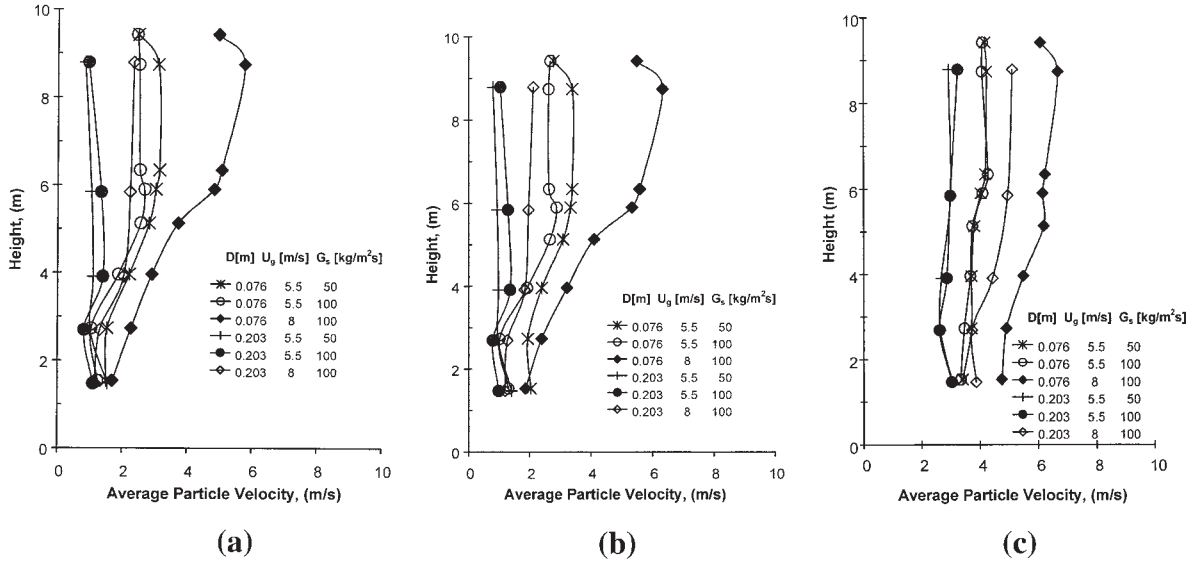

Figure 9. (a) Comparison of axial profiles of one-dimensional particle velocity in the twin-riser system: averaged from local particle velocities (weighed by local solids concentration); (b) comparison of axial profiles of one-dimensional particle velocity in the twin-riser system: deduced from the cross-sectional average solids concentration. (c) Comparison of axial profiles of one-dimensional particle velocity in the twin-riser system: averaged from local particle velocities measured at 10 radial positions (excluding the center point).

radial position to give the true cross-sectional average velocity, given that a higher solids population is typically flowing near the wall than in the center. In Figure 9b, the cross-sectionally averaged solids concentration[21] was used to calculate the average particle velocity [$=G_s/(\rho_p\bar{\varepsilon}_s)$]. The excellent agreement (with average deviation of $<10\%$) between Figure 9a and Figure 9b further confirms the reliability of the two optical-fiber probes used in this study.

In Figures 9a and 9b, the cross-sectional average particle velocity of the 203-mm ID riser is lower than that of the 76-mm ID riser under the same operating conditions, although there is no significant change for the shape of the axial profiles. That is, in terms of scale, the cross-sectional average particle velocity decreases with the riser diameter, but the shape of the axial profile changes only negligibly with the riser diameter. These correspond well to the typical axial solids holdup profiles (S-shape) of our previous study.[21] Seen from Figures 9a and 9b, increasing gas velocity obviously increases the axial particle velocities for both risers. However, changing solids fluxes appears to have no obvious influence on the axial particle velocities for both risers.

As mentioned earlier, at the same solids circulation rate and gas velocity, a larger riser has a larger solids concentration at each radial position, especially in the wall region. Thus, a larger riser has a larger cross-sectional average solids concentration at each radial position. To maintain the cross-sectional G_g, the cross-sectional average particle velocity has to be correspondingly lower in the large riser.

The large difference between the average particle velocities in the two risers may not be completely attributed to the scale, but may also be explained by the steepened radial solids distribution in the larger riser. By closely analyzing the particle velocity in each cross-section (Figure 6), it is easier to see that there is not much difference in the center region between the two risers; the 203-mm ID riser has a much lower particle velocity closer to the wall. Because more particles accumulated at the wall for the large riser (as shown in Figure 7), the weighted cross-sectional average particle velocity becomes much lower in the 203-mm ID riser. To further illustrate the point, the straight mathematic average particle velocity, without taking the weight of the radial solids distribution, were plotted in Figure 9c for the two risers. Compared with Figure 9a, the difference between the mathematic mean particle velocities of the two risers shown in Figure 9c is much smaller, suggesting that the lower local particle velocity near the wall in the larger riser is only part of the reason for the larger riser to have a lower cross-sectional average particle velocity at each axial level at the same solids circulation rate and gas velocity. In other words, the scale-up effect may not be as large as shown in Figure 9a.

In the study on the axial distributions of solids holdup, Yan and Zhu[21] reported three axial sections along the twin-riser system: the bottom dense section ($Z < 3$ m), a middle section, and a top exit section. Such a three-section structure can also be observed in the axial profiles of the cross-sectional average particle velocity shown in Figures 9a and 9b: the bottom section ($<$3–4 m), with particle velocity $<$ 2 m/s and no obvious solids acceleration; a middle section; and a top exit section.

Particle velocities vs. solids holdups

The local particle velocity at a given radial position of a certain axial level can also be directly related to the local solids concentration at the same position throughout the twin–riser system. As shown in Figure 10, the local particle velocity decreases monotonically with the local solids concentration and such a decrease follows the same pattern in all axial sections for both risers. Such a strong dependency could be understood only by considering solids aggregation at each local position: a higher solids concentration leads to stronger particle

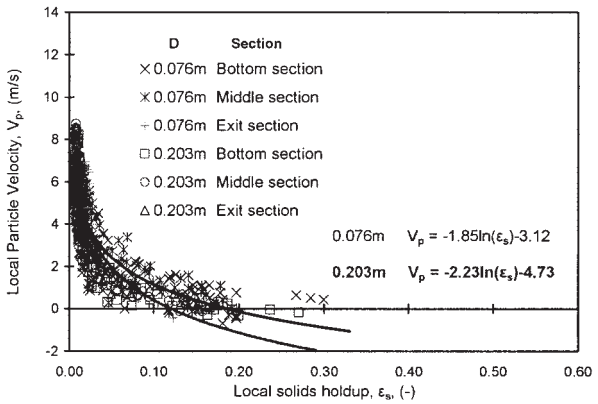

Figure 10. Relationship between local particle velocity and local solids holdup for both risers.

aggregates, resulting in a lower effective drag between the particles and gas, and therefore a lower particle velocity under a constant gas velocity. The independence of the above variation with the axial locations shows the inherent connection between the particle concentration and velocity. As a result, a single correlation works for all axial sections in each riser:

For the 76-mm ID Riser

$$V_p = -1.85\ln(\varepsilon_s) - 3.12 \quad (0 < \varepsilon_s < 0.42,\ V_p > -1.52\ \text{m/s}) \quad (2)$$

For the 203-mm ID Riser

$$V_p = -2.23\ln(\varepsilon_s) - 4.73 \quad (0 < \varepsilon_s < 0.42,\ V_p > -2.80\ \text{m/s}) \quad (3)$$

The difference between the two correlations may result from the scale-up effect as discussed above.

The average local particle velocity in the three radial sections ($0.0 < r/R < 0.632$, $0.632 < r/R < 0.894$, and $0.894 < r/R < 1.0$) can also be related to the cross-sectional mean solids holdup at a given axial position for both risers. Figures 11a and 11b show the relationship of the average local particle velocity and the cross-sectional mean solids holdup for the 76- and the 203-mm ID risers. The trends of the three regions in the 203-mm ID riser were also represented as darker lines in Figure 11a to compare with those in the 76-mm ID riser. The difference in the flow development in the three radial regions is also clearly shown in Figure 11. Similar to the case stated before in Figure 5, the particle velocities were first developed in the center region of the riser ($0.0 < r/R < 0.632$) and the particle velocities are the highest. In the middle region ($0.632 < r/R < 0.894$), on the other hand, the particle velocity is intermediate. In the wall region ($0.894 < r/R < 1.0$) the particle velocity remains low all over the riser. This again verified that the flow develops first in the center region of the riser, and then gradually and progressively closer to the wall as the solids pass through the riser. Furthermore, the scale-up effect on the flow development is also clearly observed. There is no significant difference for the two risers in the center region. In the middle region, on the other hand, the particle velocity of the 76-mm ID riser is higher than that of the 203-mm ID riser. In the wall region, the particle velocity of the 76-mm ID riser is also higher than that of the 203-mm ID riser. That is, the flow development is faster in a smaller riser diameter in these two regions. Thus, the overall flow development is slower with the large riser. These scale-up effects are the same as shown before. A clear dependency between the particle velocity and solids concentration is also shown in these figures.

Conclusions

Numerous measurements were performed in a twin-riser system to show the dependency of the particle velocity distribution and the flow development on riser diameter, using a fiber-optic probe on eight axial levels in a 10 m long riser of 76-mm and 203-mm IDs. The particle velocity is more uniform in the upper section than in the lower section of the riser at all

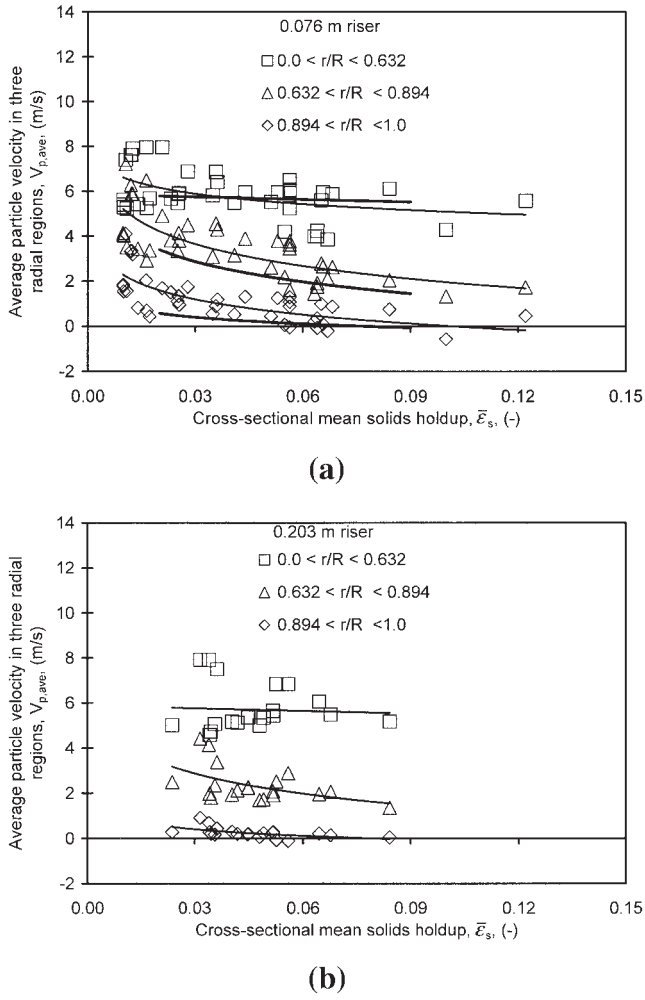

Figure 11. (a) Relationship between average particle velocity in the three radial regions and cross-sectional mean solids holdup for the 76-mm ID riser (dark line: trends for the 203-mm ID riser); (b) relationship between average particle velocity in the three radial regions and cross-sectional mean solids holdup for the 203-mm ID riser.

radial positions and is higher in the center than in the wall region of the riser at all axial locations. In the center region of the riser ($0.0 < r/R < 0.632$), the particle velocity remain high and relatively constant throughout the riser, suggesting very quick solids flow development in the riser center, and then gradually closer to the wall as the solids pass through the riser. In the middle radial region ($0.632 < r/R < 0.894$), particle velocity is increasing and continues throughout the column. In the wall region ($0.894 < r/R < 1.0$), however, the flow development is significantly slower. Furthermore, there is no significant difference for the two risers in the center region. In the middle and wall regions, on the other hand, the particle velocity of the 76-mm ID riser is higher than that of the 203-mm ID riser. The radial particle profiles change from an S-shape, in the bottom of the riser, to a combination of linear (but not flat) and parabolic shape in the middle, and eventually, parabolic with some scattering at the exit. The shape change of the radial particle profiles of the 203-mm ID riser happens at a much higher level than that of the 76-mm ID riser. The results also show at the same solids circulation rate and gas velocity, a larger-diameter riser has a steeper radial particle velocity profile at each axial level. Therefore, all the results show that the flow development slows down with larger-diameter riser.

Increasing the superficial gas velocity U_g increases the particle velocity throughout the riser length. By increasing U_g, the flow development was shown to become faster. Increasing solids flux G_s, on the other hand, slows down the flow development.

The cross-sectional average particle velocity is somewhat lower with the larger-diameter riser resulting from the scale-up effect. In all locations measured, there was a clear dependency between the local particle velocity and concentration for each riser. In addition, it is also because of the scale-up effect that the relationship between the particle velocity in the wall region and the cross-sectional solids concentration, and the correlation of the local particle velocity and solids concentration of the 203-mm ID riser are different from those of the 76-mm ID riser. More research must be done to study the riser diameter effect (D), the particle to diameter effect, a change in the dispersion and flow patterns arising from an effect at the riser inlet, or the effect of the length/diameter ratio on the development of the acceleration zone.

Gas radial distribution and particle aggregation are considered the key factors that affect the local hydrodynamics in the twin-riser system.

Acknowledgments

The authors gratefully acknowledge the financial support from the Natural Sciences and Engineering Research Council of Canada and help from J. H. Pärssinen, J. Wen, H. Zhang, and X. Zhu during the experiments.

Notation

D = riser diameter, m or inch
G_s = solids circulation rate (solids flux), kg m^{-2} s^{-1}
r = radial distance from riser axis, m
R = radius of riser, m
U_g = superficial gas velocity, m/s
V_p = particle velocity, m/s
$V_{p,ave}$ = average particle velocity in three radial regions, m/s
$V_{p,wall}$ = particle velocity in the wall region, m/s
Z = height from the riser bottom, m
$\bar{\varepsilon}_s$ = cross-sectional mean solids holdup
ε_s = local solids holdup

Literature Cited

1. Reh L. Fluidized bed processing. *Chem Eng Prog.* 1971;1:58-63.
2. Yerushalmi J, Turner DH, Squires AM. The fast fluidized bed. *I&EC Proc Des Dev.* 1976;15:47-53.
3. Bader R, Findlay J, Knowlton TM. Gas/solid flow patterns in a 30.5 cm-diameter circulating fluidized bed. In: Basu P, Large JF, eds. *Circulating Fluidized Bed Technology II.* Oxford, UK: Pergamon Press; 1988:123-137.
4. Glicksman LR. Circulating fluidized bed heat transfer. In: Basu P, Large JF, eds. *Circulating Fluidized Bed Technology II.* Oxford, UK: Pergamon Press; 1988:13-29.
5. Hartge EU, Rensner D, Werther J. Solids concentration and velocity patterns in circulating fluidized beds. In: Basu P, Large JF, eds. *Circulating Fluidized Bed Technology II.* Oxford, UK: Pergamon Press; 1988:165-180.
6. Kunii D, Levenspiel O. Entrainment of solids from fluidized beds. I. Hold-up of solids in the freeboard. II. Operation of fast fluidized beds. *Powder Technol.* 1990;61:193-206.
7. Nowak W, Mineo H, Yamazaki R, Yoshida K. Behavior of particles in a circulating fluidized bed of a mixture of two different sized particles. In: Basu P, Horio M, Hasatani M, eds. *Circulating Fluidized Bed Technology III.* Oxford, UK: Pergamon Press; 1991:219-224.
8. Bi H, Zhu JX. Static instability analysis of circulating fluidized beds and concept of high-density risers. *AIChE J.* 1993;39:1272-1280.
9. Knowlton T. Interaction of pressure and diameter on CFB pressure drop and holdup. Proc of workshop on Modeling and Control of Fluidized Bed Systems, Hamburg, Germany, May; 1995:22-23.
10. Bai D, Issangya AS, Zhu JX, Grace JR. Analysis of the overall pressure balance around a high-density circulating fluidized bed. *Ind Eng Chem Res.* 1997;36:3898-3903.
11. Issangya AS, Bai D, Bi HT, Lim KS, Zhu J, Grace JR. Axial solids holdup profiles in a high-density circulating fluidized bed riser. In: Kwauk M, Li J, eds. *Circulating Fluidized Bed Technology V.* Beijing, China: Science Press; 1996:60-65.
12. Issangya AS, Bai D, Grace JR, Lim KS, Zhu J. Flow behaviour in the riser of a high-density circulating fluidized bed. *AIChE Symp Ser.* 1997;93:25-30.
13. Issangya AS, Bai D, Bi HT, Lim KS, Zhu J, Grace JR. Suspension densities in a high-density circulating fluidized bed riser. *Chem Eng Sci.* 1999;54:5451-5460.
14. Grace JR, Issangya AS, Bai D, Bi HT, Zhu JX. Situating the high-density circulating fluidized bed. *AIChE J.* 1999;45:2108-2116.
15. Karri SBR, Knowlton TM. A comparison of annulus solids flow direction and radial solids mass flux profiles at low and high mass fluxes in a riser. In: Werther J, ed. *Circulating Fluidized Bed Technology VI.* Frankfurt, Germany: Dechema; 1999:71-76.
16. Pärssinen JH, Zhu JX. Axial and radial solids distribution in a long and high-flux CFB riser. *AIChE J.* 2001;47:2197-2205.
17. Pärssinen JH, Zhu JX. Particle velocity and flow development in a long and high-flux CFB riser. *Chem Eng Sci.* 2001;56:5295-5303.
18. Zhou J, Grace JR, Brereton C, Lim CJ. Particle velocity profiles in a circulating fluidized bed of square cross-section. *Chem Eng Sci.* 1995; 50:237-244.
19. Zhu JX, Li GZ, Qin SZ, Li FY, Zhang H, Yang YL. Direct measurements of particle velocities in gas–solids suspension flow using a novel 5-fiber optical probe. *Powder Technol.* 2001;115:184-192.
20. Zhang H, Johnston PM, Zhu JX, de Lasa HI, Bergougnou MA. A novel calibration procedure for a fibre optic concentration probe. *Powder Technol.* 1998;100:260-272.
21. Yan AJ, Zhu JX. Scale-up effect of riser reactors. (1) Axial and radial solids concentration distribution and flow development. *Ind Eng Chem Res.* 2004;43:5810-5819.

Manuscript received May 27, 2004, and revision received Mar. 14, 2005.